Journal of the Korean Society for Nondestructive Testing
Vol. 23, No. 6 (2003. 12)

A Structural Damage Identification Method Based on Spectral Element Model and Frequency Response Function

Usik Lee*,†, Seunggyu Min* and Oh-Yang Kwon*

Abstract A spectral element model-based structural damage identification method (SDIM) was derived in the previous study by using the damage-induced changes in frequency response functions. However the previous SDIM often provides poor damage identification results because the nonlinear effect of damage magnitude was not taken into account. Thus, this paper improves the previous SDIM by taking into account the nonlinear effect of damage magnitude. Accordingly an iterative solution method is used in this study to solve the nonlinear matrix equation for local damages distribution. The present SDIM is evaluated through the numerically simulated damage identification tests.

Keywords: structural damage, damage identification, spectral element model, frequency response function, nonlinearity of damage

1. Introduction

Structural damages generated within a structure may lead to the changes in the dynamic characteristics of a structure such as the vibration response, natural frequencies, mode shapes and modal damping, which in turn can be used to detect, locate and quantify the damages. Thus, a variety of structural damage identification methods (SDIMs) has been appeared in the literature.

The existing SDIMs can be classified into some groups depending on what experimental data are used in the methods. They include the changes in the modal parameters (Adams et al., 1978; Cempel et al., 1992; Griffin and Sun, 1991), strain energy (Cornwell et al., 1999), transfer function parameters (Lew, 1995), flexibility matrix (Pandey and Biswas, 1995), residual forces (Ricles and Kosmatka, 1992), wave characteristics (Feroz and Oyadiji, 1999), mechanical impedances (Wong et al., 1993), frequency response function (FRF) data (Thyagarajan, 1998) and so forth. As discussed by Banks et al. (1996), the modal-parameters-based SDIMs may have some shortcomings. First the modal data can be contaminated by measurement errors and modal extraction errors because they are indirectly measured test data. Second, the completeness of modal parameters cannot be met in most practical cases because they often require a large number of sensors. On the other hand, using measured FRF-data may have certain advantages over using the modal parameters. First the modal parameters will not be contaminated by the modal extraction errors because they are measured directly from structures. Second the FRF-data can provide much more damage information in a desired frequency range than modal parameters which are extracted from a very limited number of FRF-data around resonance (Wang et al. 1997). Thus, it seems to be very promising to use the

Received: August 16, 2003. Accepted: September 16, 2003. * Department of Mechanical Engineering, Inha University, Inchon 402-751, Korea. † Corresponding author: ulee@inha.ac.kr

FRF-data for identifying damages within a structure.

It can be found from a thorough literature survey that most SDIMs have been derived from conventional finite element model-based eigenvalue problems. As a drawback of conventional finite element method (FEM), very fine meshes should be used to obtain satisfactory dynamic solutions, especially at high frequency, which may result in significant increases of computation costs and time. In contrast with the conventional FEM, the spectral element method (SEM) is often justifiably referred to as an exact element method in the literature because it provides exact dynamic characteristics and responses by using only one finite element for a uniform structure member, regardless of its length (Doyle, 1997; Lee at al., 2000). This is possible because the exact dynamic element stiffness matrix, often called 'spectral element matrix' in the literature, is used in SEM. The exact dynamic element stiffness matrix is formulated from the frequency-dependent *exact* shape functions satisfying governing equations.

Motivated from the aforementioned advantages of the FRF-data and SEM over the modal parameters and conventional FEM, a SEM-based SDIM was derived in the authors' previous study (Lee and Shin, 2002). However, the SEM-based SDIM often provides poor damage identification results because the nonlinear effect of damage magnitude was neglected in the formulation of damage identification algorithm. Thus, a modified SEM-based SDIM is developed in this paper by taking into account the nonlinear terms with respect to damage magnitudes.

2. Modified Damage Identification Algorithm

The dynamic stiffness equation for a structure in the intact state can be represented by (Lee and Shin, 2002)

$$[\mathbf{S}(\omega)]\{\mathbf{U}(\omega)\}=\{\mathbf{P}(\omega)\} \tag{1}$$

where ω is the circular frequency and [S] and {U} are the dynamic stiffness matrix and the spectral components of the nodal degrees of freedom vector (simply, nodal DOFs vector) of the intact structure, respectively. Note that the dynamic stiffness matrix is frequency-dependent. The vector {P} is the spectral components of the external nodal forces vector (simply, nodal forces vector). Assuming the structure gets damaged, but still subjected to the same nodal forces as in Eq. (1), the dynamic stiffness equation for the structure in the damaged state can be represented by

$$[\bar{\mathbf{S}}(\omega)]\{\bar{\mathbf{U}}(\omega)\}=\{\mathbf{P}(\omega)\} \tag{2}$$

where $[\bar{\mathbf{S}}]$ and $\{\bar{\mathbf{U}}\}$ are the dynamic stiffness matrix and the spectral nodal DOFs vector for damaged structure, respectively.

In this study, the matrix [S] is considered as the known quantity because it will be so determined that Eq. (1) represents the refined structure model for the intact structure. By the word 'refined', we mean that the experimentally measured and analytically predicted structural dynamic characteristics are in good agreement. The (spectral) nodal DOFs vector $\{\bar{\mathbf{U}}\}$ is also considered as a known quantity because it will be measured directly from the damaged structure in practice. However the matrix $[\bar{\mathbf{S}}]$ is not known in advance because it will depend on the not-yet-known current state of damage. Assume the matrix $[\bar{\mathbf{S}}]$ can be expressed in the form

$$[\bar{\mathbf{S}}(\omega)]=[\mathbf{S}(\omega)]+[\Delta\mathbf{S}(\omega)] \tag{3}$$

where $[\Delta\mathbf{S}]$ is the perturbed dynamic stiffness matrix generated by the presence of damage. Substituting Eq. (3) into Eq. (2) gives

$$\{\mathbf{P}(\omega)\}-[\mathbf{S}(\omega)]\{\bar{\mathbf{U}}(\omega)\}=[\Delta\mathbf{S}(\omega)]\{\bar{\mathbf{U}}(\omega)\} \tag{4}$$

The nodal forces vector {P} can be written in the partitioned-vector form as

$$\{\mathbf{P}(\omega)\}=\begin{Bmatrix}\mathbf{P}_m(\omega)\\ \mathbf{P}_s(\omega)\end{Bmatrix}=\begin{Bmatrix}\mathbf{F}(\omega)\\ \mathbf{0}\end{Bmatrix} \tag{5}$$

where $\{\mathbf{0}\}$ denotes the null vector. In a manner compatible with Eq. (5), the vector $\{\bar{\mathbf{U}}\}$ can be partitioned into a set $\{\bar{\mathbf{U}}_m\}$ termed 'master' nodal DOFs vector, which is to be retained, and a set $\{\bar{\mathbf{U}}_s\}$ termed 'slave' nodal DOFs vector, which are to be eliminated to reduce the number of nodal DOFs as follows:

$$\{\bar{\mathbf{U}}(\omega)\} = \begin{Bmatrix} \bar{\mathbf{U}}_m(\omega) \\ \bar{\mathbf{U}}_s(\omega) \end{Bmatrix} \tag{6}$$

Similarly, the matrices $[\mathbf{S}]$ and $[\bar{\mathbf{S}}]$ can be expressed in the forms

$$[\mathbf{S}(\omega)] = \begin{bmatrix} \mathbf{S}_{mm}(\omega) & \mathbf{S}_{ms}(\omega) \\ \mathbf{S}_{sm}(\omega) & \mathbf{S}_{ss}(\omega) \end{bmatrix} \tag{7}$$

$$[\bar{\mathbf{S}}(\omega)] = \begin{bmatrix} \bar{\mathbf{S}}_{mm}(\omega) & \bar{\mathbf{S}}_{ms}(\omega) \\ \bar{\mathbf{S}}_{sm}(\omega) & \bar{\mathbf{S}}_{ss}(\omega) \end{bmatrix} \tag{8}$$

By substituting Eqs. (5), (6) and (8) into Eq. (2), the nodal DOFs vector $\{\bar{\mathbf{U}}\}$ can be expressed in terms of $\{\bar{\mathbf{U}}_m\}$ only as follows:

$$\{\bar{\mathbf{U}}(\omega)\} = [\bar{\mathbf{T}}(\omega)]\{\bar{\mathbf{U}}_m(\omega)\} \tag{9}$$

where $[\bar{\mathbf{T}}(\omega)]$ is the coordinates transformation matrix for damaged structure, given by

$$[\bar{\mathbf{T}}(\omega)] = [\mathbf{T}(\omega)] + [\Delta\mathbf{T}(\omega)] \tag{10}$$

where

$$[\mathbf{T}(\omega)] = \begin{bmatrix} \mathbf{I} \\ \mathbf{t}(\omega) \end{bmatrix}, \quad [\Delta\mathbf{T}(\omega)] = \begin{bmatrix} \mathbf{0} \\ \Delta\mathbf{t}(\omega) \end{bmatrix} \tag{11}$$

$$[\mathbf{t}(\omega)] = -[\mathbf{S}_{ss}]^{-1}[\mathbf{S}_{sm}] \tag{12}$$

$$[\Delta\mathbf{t}(\omega)] = [\mathbf{C}_{ss}][\mathbf{t}] + [\mathbf{t}][\mathbf{C}_{sm}] + [\mathbf{C}_{ss}][\mathbf{t}][\mathbf{C}_{sm}] \tag{13}$$

$$[\mathbf{C}_{ss}] = -[\mathbf{S}_{ss}]^{-1}[\Delta\mathbf{S}_{ss}]([\mathbf{I}] + [\mathbf{S}_{ss}]^{-1}[\Delta\mathbf{S}_{ss}])^{-1} \tag{14}$$

$$[\mathbf{C}_{sm}] = [\mathbf{S}_{sm}]^{-1}[\Delta\mathbf{S}_{sm}] \tag{15}$$

Substituting Eq. (10) into Eq. (9) and then into Eq. (4), and applying Eqs. (5), (7) and (11) yields

$$\{\boldsymbol{\delta}\} + \frac{1}{\omega^2}[\mathbf{X}(\omega)]\{\mathbf{A}_m(\omega)\} = -\frac{1}{\omega^2}[\mathbf{Y}(\omega)]\{\mathbf{A}_m(\omega)\} \tag{16}$$

where

$$[\mathbf{X}(\omega)] = [\mathbf{S}_{mm}] + [\mathbf{S}_{ms}][\mathbf{t}] \tag{17}$$

$$\begin{aligned}[\mathbf{Y}(\omega)] = {} & ([\mathbf{S}_{ms}] + [\Delta\mathbf{S}_{ms}])[\mathbf{S}_{ss}]^{-1}[\Delta\mathbf{S}_{ss}]([\mathbf{S}_{ss}] + [\Delta\mathbf{S}_{ss}])^{-1}([\mathbf{S}_{sm}] + [\Delta\mathbf{S}_{sm}]) \\ & - ([\mathbf{S}_{ms}] + [\Delta\mathbf{S}_{ms}])[\mathbf{S}_{ss}]^{-1}[\Delta\mathbf{S}_{sm}] + [\Delta\mathbf{S}_{mm}] - [\Delta\mathbf{S}_{ms}][\mathbf{S}_{ss}]^{-1}[\mathbf{S}_{sm}]\end{aligned} \tag{18}$$

In Eq. (16), $\{\mathbf{A}_m\}$ is the inertance FRF, which is defined as the ratio of the acceleration to the applied force (Ewins, 1984), and $\{\delta\}$ is the nodal forces locator vector that has unit values at the components corresponding to non-zero nodal forces.

The matrix $[\mathbf{Y}(\omega)]$ defined by Eq. (18) is the nonlinear function of unknown damage magnitudes and can be expressed as the sum of the linear part $[\mathbf{Y}_0]$ and the nonlinear part $[\mathbf{Y}_{NL}]$ as follows:

$$[\mathbf{Y}(\omega)] = [\mathbf{Y}_0(\omega)] + [\mathbf{Y}_{NL}(\omega)] \tag{19}$$

where

$$[\mathbf{Y}_0(\omega)] = [\mathbf{T}]^T[\Delta\mathbf{S}][\mathbf{T}] \tag{20}$$

$$[\mathbf{Y}_{NL}(\omega)] = [\mathbf{Y}(\omega)] - [\mathbf{Y}_0(\omega)] \tag{21}$$

In the previous study by Lee and Shin (2002), the nonlinear part $[\mathbf{Y}_{NL}]$ was neglected by assuming local damages are small enough. This approximation is often found to provide poor damage identification results. Thus, in this study, the nonlinear part $[\mathbf{Y}_{NL}]$ will be retained to obtain an improved damage identification algorithm.

The dynamic stiffness matrix $[\mathbf{S}]$ for a complete structure can be obtained by assembling all dynamic element stiffness matrices as follows:

$$[\mathbf{S}(\omega)] = \sum_{k=1}^{N}[\mathbf{L}_k]^T[\mathbf{s}_k(\omega)][\mathbf{L}_k] \tag{22}$$

where N is the number of finite element and $[\mathbf{s}_k]$ is the dynamic element stiffness matrix for the kth finite element. The matrix $[\mathbf{L}_k]$ is the locator matrix which locates the components of $[\mathbf{s}_k]$ into

[S] for the assembly. Similarly the perturbed dynamic stiffness matrix [ΔS] can be obtained from

$$[\Delta S(\omega)] = \sum_{k=1}^{N} [L_k]^T [\Delta s_k(\omega)][L_k] \qquad (23)$$

where [Δs_k] is the perturbed dynamic element stiffness matrix for the kth finite element. As discussed in the previous work (Lee and Shin, 2002), by representing a finite element having non-uniform local damages inside as the finite element with effective uniform damage through the whole finite element, the perturbed dynamic element stiffness matrix [Δs_k] can be approximated as

$$[\Delta s_k(\omega)] \cong D_k [s_k(\omega=0)] = -D_k [k_k] \qquad (24)$$

where [k_k] and D_k are the conventional finite element stiffness matrix and effective uniform damage magnitute for the the kth finite element, respectively.

By using Eqs. (19) through (21) and (23), the right-hand side of Eq. (16) can be expressed as

$$RHS\ of\ Eq.(16) = [\Phi(\omega)]\{D\} + \{R(\omega, D)\} \qquad (25)$$

where

$$[\Phi(\omega)] = [\ \varphi_1(\omega)\ \ \varphi_2(\omega)\ \ \ldots\ \ \varphi_N(\omega)]$$
$$\{D\} = \{D_1\ \ D_2\ \ \ldots\ \ D_N\}^T$$
$$\{R(\omega, D)\} = -\frac{1}{\omega^2}[Y_{NL}(\omega, D)]\{A_m(\omega)\}$$
$$\{\varphi_k(\omega)\} = -\frac{1}{\omega^2}([L_k][T(\omega)])^T[k_k]([L_k][T(\omega)])\{A_m(\omega)\} \qquad (26)$$

Finally, replacing the right-hand side of Eq. (16) with the expression of Eq. (25) gives

$$[\Phi(\omega)]\{D\} = \{B(\omega)\} - \{R(\omega, D)\} \qquad (27)$$

where

$$\{B(\omega)\} = \{\delta\} + \frac{1}{\omega^2}[X(\omega)]\{A_m(\omega)\} \qquad (28)$$

Equation (27) represents the matrix equation for the modified structural damage identification algorithm to be used in the present study. The nonlinear terms with respect to damage magnitudes are retained in the vector {R}.

Because the vector {R} is the nonlinear function of the unknown damage magnitudes vector {D}, Eq. (27) is certainly a nonlinear matrix equation for the damage magnitudes vector {D}. Accordingly, a direct iteration method shown in Fig. 1 is used in this study to solve Eq. (27) for {D}. The damage magnitudes solved from the linearized matrix equation, which can be derived from Eq. (27) by simply neglecting the nonlinear term {R}, are used as the initial guess of {D} required to initiate the iterative computation.

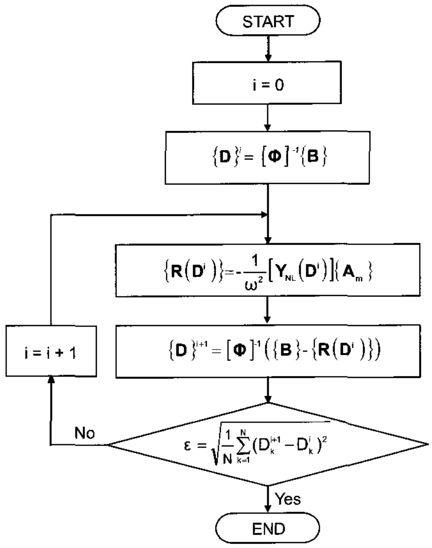

Fig. 1 A direct iterative solution procedure used for the present structural damage identification method

The convergence of predicted damage is measured by using the parameter ε which is defined as the root mean squared (RMS) value of the differences between the results obtained at the previous and current iteration steps. In Fig. 1, N denotes the total number of finite elements used in the damage identification analysis, D_k is the predicted damage magnitude in the kth finite element, and the superscript i represents the ith step of iteration. The iteration will be stopped when the value of ε becomes less than a pre-specified small limit value.

To measure the accuracy of the predicted damage magnitudes, the damage identification error (DIE) defined by

$$\mathrm{DIE} \equiv \sqrt{\frac{1}{L}\sum_{j=1}^{N} l_j \left(D_j^{Pred} - D_j^{True}\right)^2} \qquad (29)$$

is used. In Eq. (29), L is the length of beam, D_j is the damage magnitude in the jth finite element of length l_j, the superscripts '*True*' and '*Pred*' denote the true damage values and predicted values, respectively. Accordingly, as the value of DIE becomes smaller, the predicted damage state is getting closer to the true state.

3. Numerical Results and Discussion

To evaluate the feasibility of the present modified SDIM, compared with the previous linear version of SDIM (Lee and Shin, 2002), a cantilevered Euler-beam as shown in Fig. 2 is considered as an illustrative example. The beam has the length L = 0.4m, the bending rigidity EI = 14.6N-m^2, and the mass density per length ρA = 0.275kg/m. When the beam is considered to be divided into 81 equal sized finite elements, three local damages having magnitudes D_1 = 0.4, D_2 = 0.5, and D_3 = 0.3 are assumed to be located at the 14th, 41st, and 68th finite elements from the clamped root, and then the present and previous damage identification methods are applied to inversely identify them. The dynamic element stiffness matrix for the intact Euler beam, which is required in Eq. (27), is given by (Doyle, 1997; Lee et al, 2000)

$$[s(\omega)] = \frac{\kappa EI}{Ch \cdot c - 1}\begin{bmatrix} s_1 & s_2 \\ s_2^T & s_3 \end{bmatrix} \qquad (30)$$

where

$$[s_1] = \begin{bmatrix} -\kappa^2(Ch\cdot s + Sh\cdot c) & -\kappa \cdot Sh \cdot s \\ -\kappa\cdot Sh\cdot s & -(Ch\cdot s - Sh\cdot c) \end{bmatrix}$$

$$[s_2] = \begin{bmatrix} \kappa^2(Sh + s) & -\kappa(Ch - c) \\ \kappa(Ch - c) & -(Sh - s) \end{bmatrix} \qquad (31)$$

$$[s_3] = \begin{bmatrix} -\kappa^2(Ch\cdot s + Sh\cdot c) & \kappa\cdot Sh\cdot s \\ \kappa\cdot Sh\cdot s & -(Ch\cdot s - Sh\cdot c) \end{bmatrix}$$

with the use of following definitions

$$s = \sin\kappa l,\ c = \cos\kappa l,\ Sh = \sinh\kappa l,\ Ch = \cosh\kappa l \qquad (32)$$

Table 1 compares the natural frequencies before and after damage. In general, the local damages are found to reduce the natural frequencies in magnitude due to the degradation of structural stiffness. In Fig. 3, the inertance FRF measured at x = $L/3$ in the intact state is compared with that measured in the damaged state. Figure 3 shows that local damages shift the resonance peaks to the lower frequencies, which can be readily expected from Table 1.

Table 1 Damage-induced changes in the natural frequencies (Hz)

Modes	Intact	Damaged	% decrease
1st	25.70	25.38	1.24
2nd	161.08	157.18	2.42
3rd	451.04	449.55	0.33
4th	883.85	865.22	2.10
5th	1461.07	1442.45	1.27

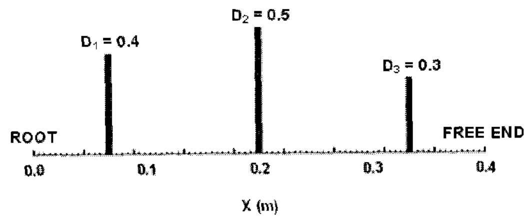

Fig. 2 Example problem for the numerical tests of the present structural damage identification method

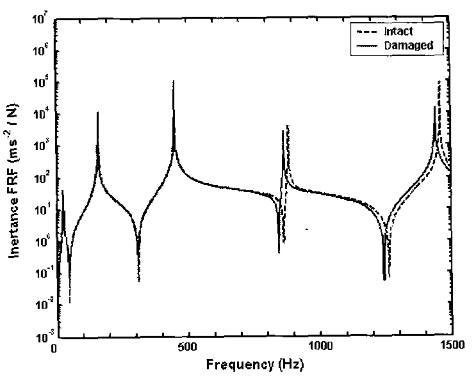

Fig. 3 Inertance frequency response functions at x = 0.133m; ...., the intact state; ______, the damaged state

Table 2 shows how the predicted damage magnitudes, parameter ε and the value of DIE vary as the number of iteration s is increased. In Table 1, the damage magnitudes given in the first row are the initial guesses of damage magnitudes, which are obtained by using the linear SDIM. It is shown that, as the number of iterations is increased up to fifteen, the predicted damage magnitudes almost converge to the true values, while ε and DIE are decreased to the values very close to zero. Using the damage magnitudes predicted by the linear SDIM as the initial guesses (for iterative damage identification process) is found to provide converged satisfactory damage identification results.

Table 2 Convergence of the damage identification results

Iteration	Damage Magnitudes			ε	DIE
	D_1	D_2	D_3		
Initial	0.469	0.612	0.335	-	2.07×10^{-2}
1st	0.371	0.435	0.293	3.71×10^{-2}	1.70×10^{-2}
2nd	0.410	0.530	0.300	2.60×10^{-2}	9.14×10^{-3}
3rd	0.396	0.485	0.300	1.45×10^{-2}	5.40×10^{-3}
7th	0.400	0.499	0.300	1.28×10^{-3}	3.81×10^{-4}
15th	0.400	0.500	0.300	5.31×10^{-6}	1.69×10^{-6}

In Fig. 4, the damage identification results obtained by using the present SDIM are compared with those obtained by using the previous linear SDIM (Lee and Shin, 2002). To compute the inertance FRF in the damaged state, the exciting frequency is chosen as 25Hz. Figure 4 certainly shows that the present SDIM predicts quite accurate damage magnitudes (0.40, 0.50, 0.30) at three damaged sites when compared with the predictions (0.47, 0.61, 0.33) by the previous linear SDIM (Lee and Shin, 2002). This improvement of damage identification is mainly attributed to including the nonlinear effects of damage magnitudes in the present improved SIDM. Additional damage identification tests for different excitation frequencies also show that the present SDIM is much superior to the previous linear SDIM (Lee and Shin, 2002). It is also found that, when compared with the previous linear SDIM, the present SDIM is less sensitive to the choice of excitation frequency even though the damage identification results are slightly dependent on the chosen excitation frequency.

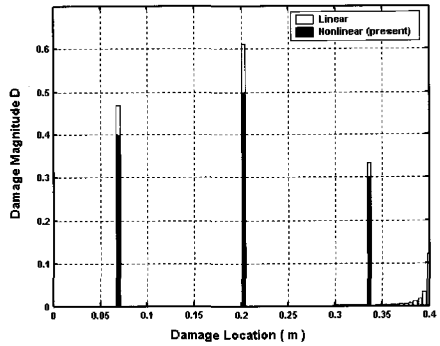

Fig. 4 Comparison of the damage identification results obtained by the present nonlinear method and the previous linear method (Lee and Shin, 2002)

4. Conclusion

An improved FRF-data/SEM-model based SDIM is developed by taking into account the nonlinear effect of damage magnitude, which was neglected in the previous work. The present SDIM is then evaluated through an illustrative example problem: a cantilevered Euler-beam with three local damages. First, it is shown that natural frequencies are decreased in magnitude due to the presence of damages. Through the numerically simulated damage identification tests, it is then proved that the present SDIM is much superior to the previous linear SDIM for identifying the pre-specified local damages and that it is less sensitive to the choice of excitation frequency. An experimental study to verify the present SDIM as well as to confirm the above results will be in the due course.

Acknowledgement

This work was supported by Korea Research Foundation Grant (KRF-2002-041-D00013).

References

Adams, R. D., Cawley, P., Pye, C. J. and Stone, B. J. (1978) A Vibration Technique for Non-destructively Assessing the Integrity of Structures, Journal of Mechanical Engineering Science, Vol. 20, No. 2, pp. 93-100

Banks, H. T., Inman, D. J., Leo, D. J. and Wang, Y. (1996) An Experimentally Validated Damage Detection Theory in Smart Structures, Journal of Sound and Vibration, Vol. 191, No. 5, pp. 859-880

Cempel, C., Matkem, H. G. and Ziolkowski, A. (1992) Application of Transformed Normal Modes for Damage Location in Structures, pp. 246-255, Structural Integrity Assessment, Elsevier, Oxford

Cornwell, P., Doebling, S. W. and Farrar, C. R. (1999) Application of the Strain Energy Damage Detection Method to Plate-like Structures, Journal of Sound and Vibration, Vol. 224, No. 2, pp. 359-374

Doyle, J. F. (1997) Wave Propagation in Structures: Spectral Analysis Using Fast Discrete Fourier Transforms, Springer-Verlag, New York

Ewins, D. J. (1984) Modal Testing: Theory and Practice, Research Studies Press, Hertfordshire

Feroz, K. T. and Oyadiji, S. O. (1999) Damage Detection in Rods Using Wave Propagation and Regression Analysis, Proceedings of the 1999 ASME Design Engineering Technical Conferences, NV, DETC99/VIB-8372, Las Vegas

Griffin, S. F. and Sun, C. T. (1991) Health Monitoring of Dumb and Smart Structures, Proceedings of the 28th Annual Technical Meeting of SES

Lee, U., Kim, J. and Leung, A. Y. T. (2000) The Spectral Element Method in Structural Dynamics, The Shock and Vibration Digest, Vol. 32, No. 6, pp. 451-465

Lee, U. and Shin, J. (2002) A Frequency-Domain Method of Structural Damage Identification Formulated from the Dynamic Stiffness Equation of Motion, Journal of Sound and Vibration, Vol. 257, No. 4, pp. 615-634

Lew, J. S. (1995) Using Transfer Function Parameter Changes for Damage Detection of Structures, AIAA Journal, Vol. 33, No. 11, pp. 2189-2193

Pandey, A. K. and Biswas, M. (1995) Damage Diagnosis of Truss Structures by Estimation of Flexibility Change, International Journal of Analytical and Experimental Modal Analysis, Vol. 10, No. 2, pp. 104-117

Ricles, J. M. and Kosmatka, J. B. (1992) Damage Detection in Elastic Structures Using Vibratory Residual Forces and Weighted Sensitivity, AIAA Journal, Vol. 30, No. 9, pp. 2310-2316

Thyagarajan, S. K., Schulz, M. J. and Pai, P. F. (1998) Detecting Structural Damage Using Frequency Response Functions, Journal of Sound and Vibration, Vol. 210, No. 1, pp. 162-170

Wang, Z., Lin, R. M. and Lim, M. K. (1997) Structural Damage Detection Using Measured FRF Data, Computer Methods in Applied Mechanics and Engineering, Vol. 147, pp. 187-197

Wong, B. S, Guan, T. C. and King, L. M. (1993) Mechanical Impedance Inspection of Composite Structures, British Journal of NDT Vol. 35, pp. 3-9